

# A deep ALMA image of the Hubble Ultra Deep Field

J.S. Dunlop et al. submitted to MNRAS

Presented by H. Umehata

# Abstract

## ABSTRACT

We present the results of the first, deep ALMA imaging covering the full  $\simeq 4.5 \text{ arcmin}^2$  of the Hubble Ultra Deep Field (HUDF) as previously imaged with WFC3/IR on the *HST*. Using a mosaic of 45 ALMA pointings, we have obtained a homogeneous image of the HUDF at  $\lambda = 1.3 \text{ mm}$ , achieving an rms sensitivity  $\sigma_{1.3} \simeq 35 \mu\text{Jy}$ , at a resolution of  $\simeq 0.7 \text{ arcsec}$ . From an initial list of  $\simeq 50 > 3.5\sigma$  peaks, a rigorous analysis confirms 16 sources with flux densities  $S_{1.3} > 120 \mu\text{Jy}$ . All of these have secure galaxy counterparts with robust redshifts ( $\langle z \rangle = 2.15$ ), and 12 are also detected at 6 GHz in new ultra-deep JVLA imaging. Due to the wealth of supporting data in this unique field, the physical properties of the ALMA sources are well constrained, including, crucially, their stellar masses ( $M_*$ ) and UV+FIR star-formation rates (SFR). Our results show that stellar mass is the best predictor of SFR in the high-redshift Universe; indeed at  $z \geq 2$  our ALMA sample contains 7 of the 9 galaxies in the HUDF with  $M_* \geq 2 \times 10^{10} M_\odot$ , and we detect only one galaxy at  $z > 3.5$ , reflecting the rapid drop-off of high-mass galaxies with increasing redshift. The detected sources, coupled with stacking, allow us to probe the redshift/mass distribution of the 1.3-mm background down to  $S_{1.3} \simeq 10 \mu\text{Jy}$ . We find strong evidence for a steep ‘main sequence’ for star-forming galaxies at  $z \simeq 2$ , with  $\text{SFR} \propto M_*$  and a mean specific  $\text{SFR} \simeq 2.2 \text{ Gyr}^{-1}$ . Moreover, we find that  $\simeq 85\%$  of total star formation at  $z \simeq 2$  is enshrouded in dust, with  $\simeq 65\%$  of all star formation at this epoch occurring in high-mass galaxies ( $M_* > 2 \times 10^{10} M_\odot$ ), for which the average obscured:unobscured SF ratio is  $\simeq 200$ . Finally, we combine our new ALMA results with the existing *HST* data to revisit the cosmic evolution of star-formation rate density ( $\rho_{\text{SFR}}$ ); we find that  $\rho_{\text{SFR}}$  peaks at  $z \simeq 2.5$ , and that the star-forming Universe transits from primarily unobscured to primarily obscured thereafter at  $z \simeq 4$ .

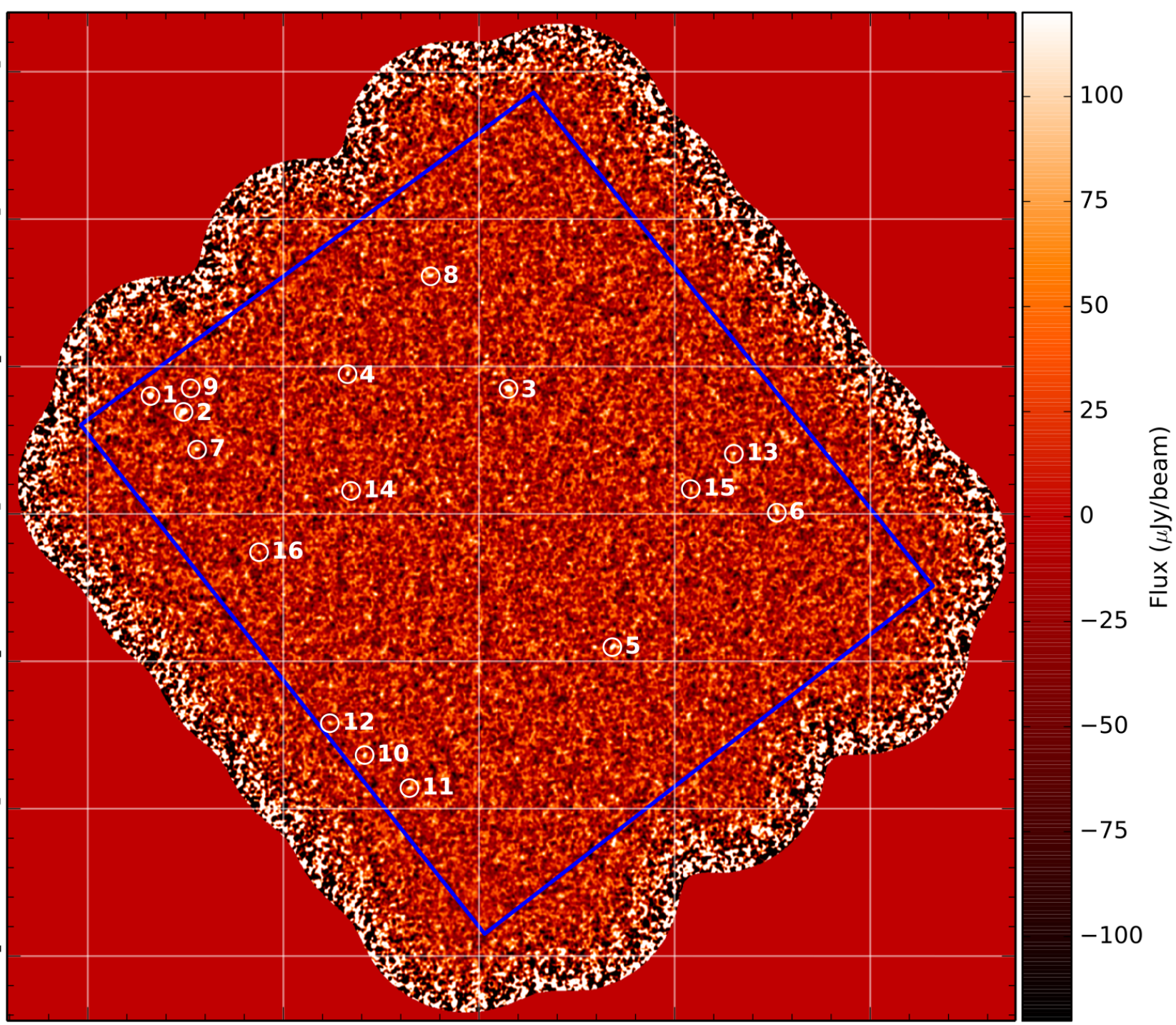
# ALMA Observations

## § Observations

- 13 days in 2014-2015
- Max baseline: 550-1250 m
- 45-pointing mosaic (separated by x0.8 antenna beam)
  - one SB terminated after 20 pointing -> included.

## § Reduction and Imaging

- standard procedures using CASA
- CLEAN with natural weighting:
  - > synthesized beam:  $589 \times 503 \text{ mas}^2$
- A  $220 \times 180 \text{ k}\lambda$  taper:
  - >  $\sim$ requested beam:  $707 \times 672 \text{ mas}^2$
- final mosaic sensitivity at center: 34 uJy/beam
- no deconvolution.



# Other wavelength data

## § Optical/NIR $5\sigma$ depth

- ACS: B,V,I,z -> 29.7, 30.2, 29.9, 29.8
- WFC3: Y,J125,J140,H160 -> 29.7, 29.2, 29.2, 29.2
- HAWK-I: K<sub>s</sub> -> 26.5

## § Other data

- Spitzer / Herschel
  - > ‘we fitted the Herschel maps with appropriate beams at the ALMA source positions’
- Radio: rms 0.32 uJy/beam at 6 GHz
  - > 27 radio sources with  $>5\sigma$
- MUSE: 3x3 mosaic of 18.2 ksec (+ 65 ksec in the centre)
  - > detected line(s) for 6/16 ALMA sources
  - > 4/6 are new.

# ALMA Source Extraction

## § Method

- create ‘noise’ map
  - > evaluated the standard deviation for each pixel.
- then make ‘SNR’ map
- Search and Destroy. (AIPS/SAD-like?)

## § Survey area

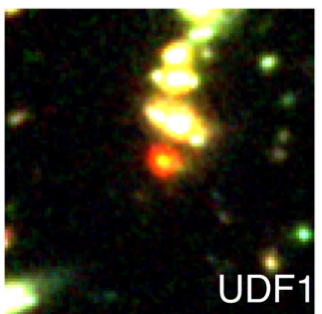
- 4.4 arcmin<sup>2</sup> with  $\sigma < 40$  uJy (Cf. 34 uJy at centre)
- positive: 47 sources with  $\geq 3.5\sigma$   
negative: 29 sources with  $\geq 3.5\sigma$   
 $\Rightarrow$  15-20 sources would be real.

(...counts as a function of SNR?)

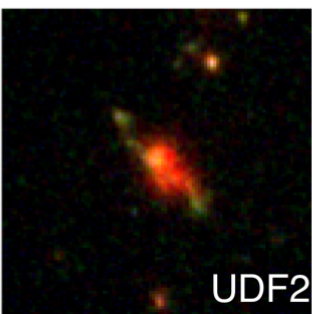
- 5 sources with  $6\sigma$  are ‘secure’
- 7 ‘negative’ sources with  $4\sigma$

# ALMA Source Catalog

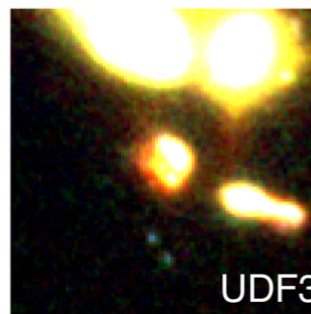
ID	RA (ALMA) /deg	Dec (ALMA) /deg	$S_{1.3\text{mm}}$ / $\mu\text{Jy}$	S/N 1.3mm	RA ( <i>HST</i> ) /deg	Dec ( <i>HST</i> ) /deg	$\Delta_1$ /arcsec	$\Delta_2$ /arcsec	$H_{160}$ /ABmag	$z$	Ref
UDF1	53.18348	−27.77667	$924 \pm 76$	18.37	53.18345	−27.77658	0.33	0.13	24.75	3.00	
UDF2	53.18137	−27.77757	$996 \pm 87$	16.82	53.18140	−27.77746	0.38	0.15	24.70	2.794	1
UDF3	53.16062	−27.77627	$863 \pm 84$	13.99	53.16060	−27.77613	0.51	0.27	23.41	2.541	2
UDF4	53.17090	−27.77544	$303 \pm 46$	6.63	53.17090	−27.77539	0.18	0.06	24.85	2.43	
UDF5	53.15398	−27.79087	$311 \pm 49$	6.33	53.15405	−27.79091	0.24	0.42	23.30	1.759	3
UDF6	53.14347	−27.78327	$239 \pm 49$	4.93	53.14347	−27.78321	0.22	0.03	22.27	1.411	2
UDF7	53.18051	−27.77970	$231 \pm 48$	4.92	53.18052	−27.77965	0.21	0.06	24.17	2.59	
UDF8	53.16559	−27.76990	$208 \pm 46$	4.50	53.16555	−27.76979	0.43	0.22	21.75	1.552	4
UDF9	53.18092	−27.77624	$198 \pm 39$	4.26	53.18105	−27.77617	0.46	0.40	21.41	0.667	2
UDF10	53.16981	−27.79697	$184 \pm 46$	4.02	53.16969	−27.79702	0.42	0.56	23.32	2.086	3
UDF11	53.16695	−27.79884	$186 \pm 46$	4.02	53.16690	−27.79869	0.54	0.31	21.62	1.996	2, 4
UDF12	53.17203	−27.79517	$154 \pm 40$	3.86	53.17212	−27.79509	0.39	0.28	27.00	5.000	5
UDF13	53.14622	−27.77994	$174 \pm 45$	3.85	53.14615	−27.77988	0.31	0.24	23.27	2.497	3
UDF14	53.17067	−27.78204	$160 \pm 44$	3.67	53.17069	−27.78197	0.24	0.06	22.76	0.769	2
UDF15	53.14897	−27.78194	$166 \pm 46$	3.56	53.14902	−27.78196	0.18	0.36	23.37	1.721	3
UDF16	53.17655	−27.78550	$155 \pm 44$	3.51	53.17658	−27.78545	0.22	0.09	21.42	1.314	2, 6



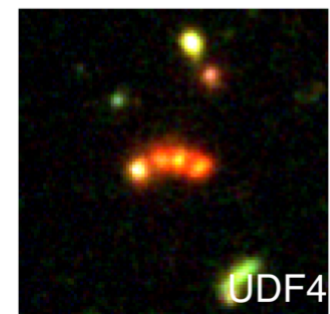
UDF1



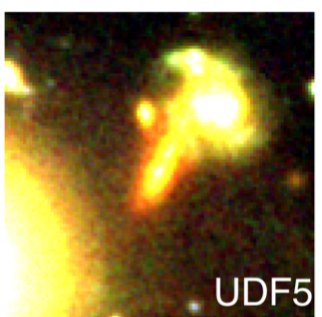
UDF2



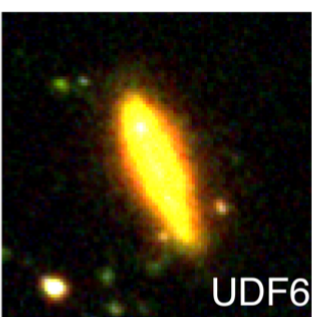
UDF3



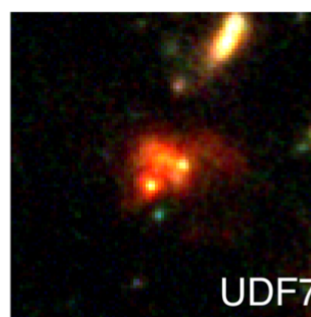
UDF4



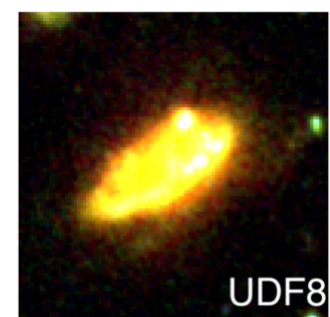
UDF5



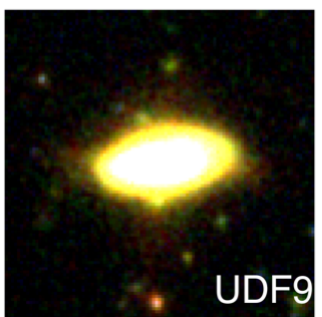
UDF6



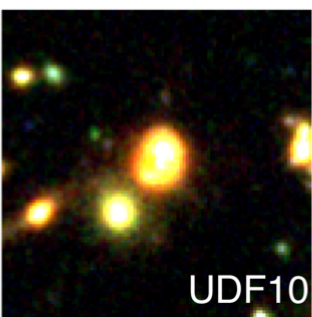
UDF7



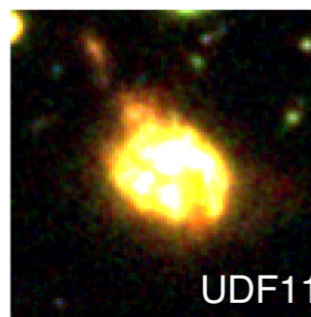
UDF8



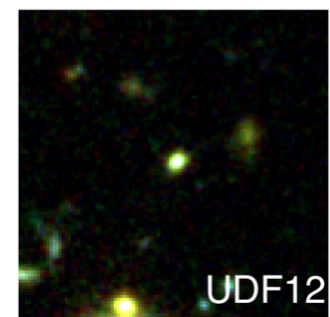
UDF9



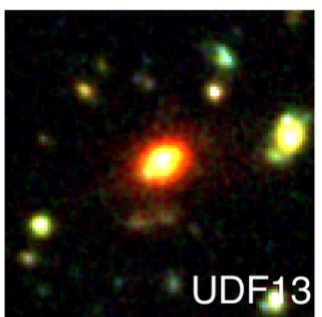
UDF10



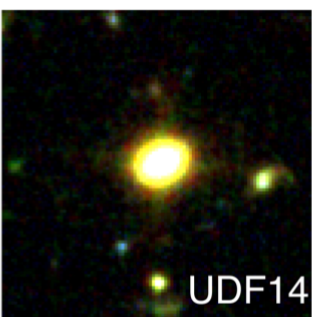
UDF11



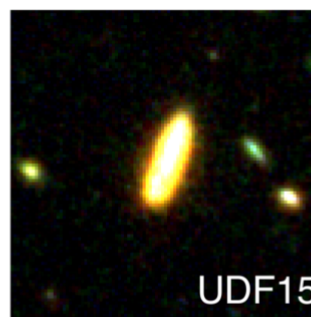
UDF12



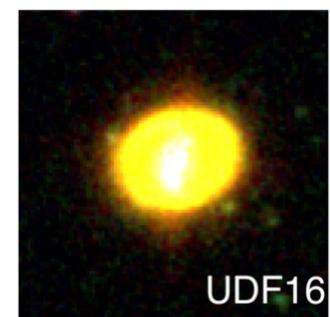
UDF13



UDF14



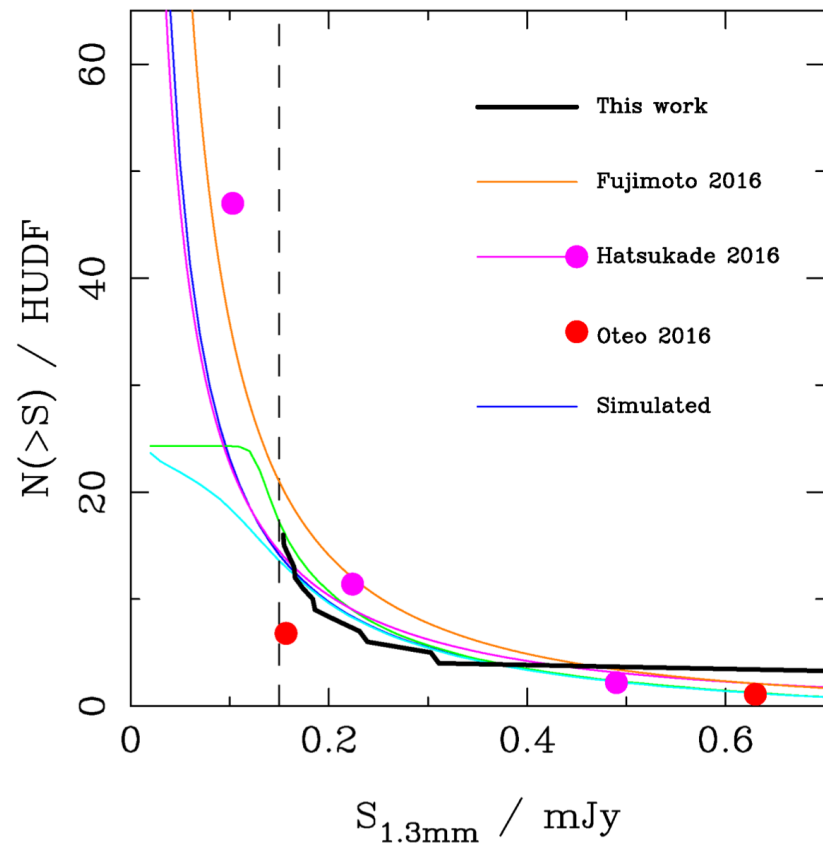
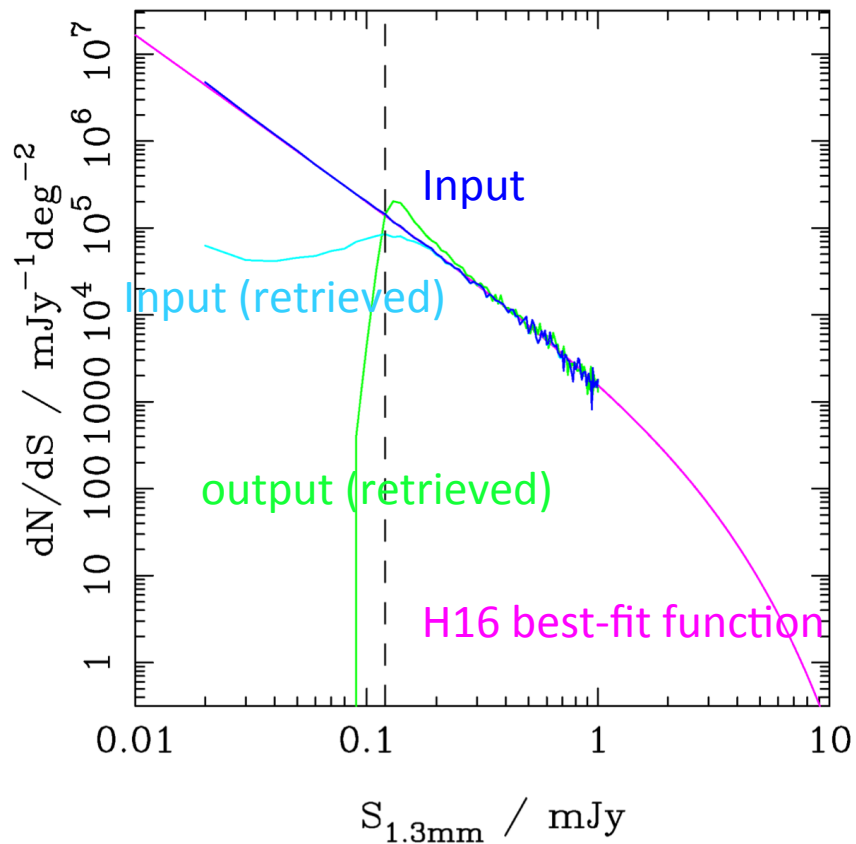
UDF15



UDF16

i+Y+H  
6''x6''

# Number Counts



- ‘in very good agreement with integration of the Schechter function of H16’.
- significant work still needs to be done to clarify the faint-end.

# Properties

↓ SED Fit

Chabrier IMF

↓ SED Fit ↓

↓ Multiple Templates

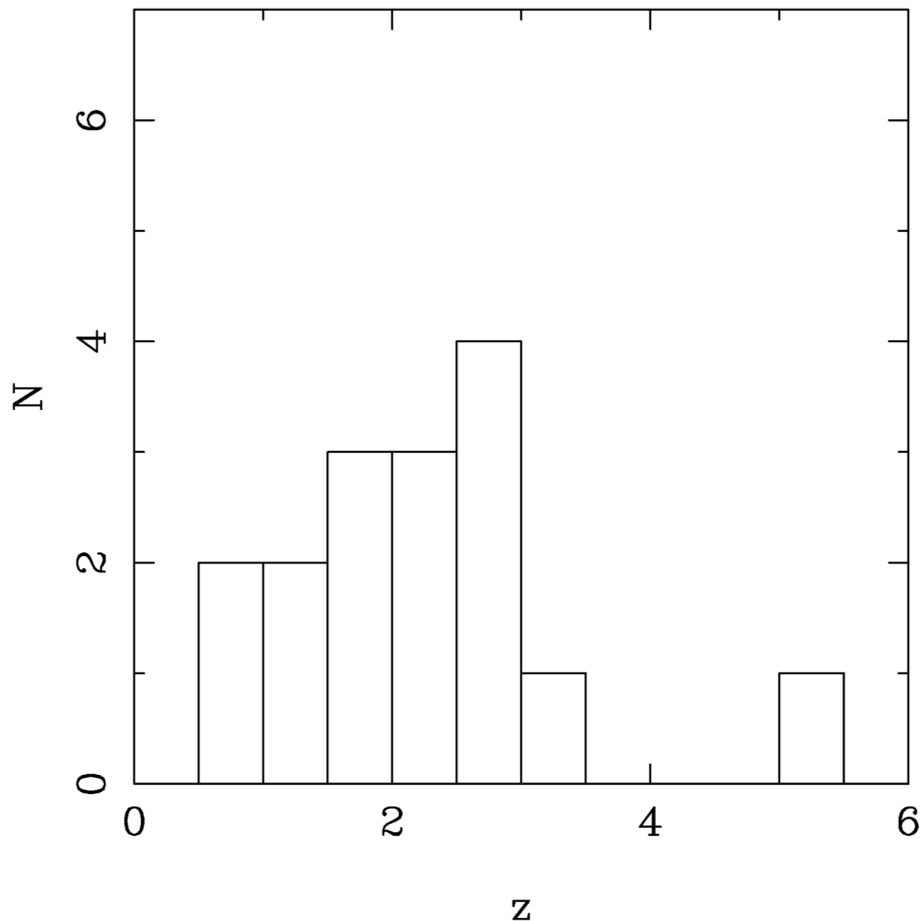
ID	$\log_{10}(M_*/M_\odot)$	SFR <sub>UV</sub> $/M_\odot \text{yr}^{-1}$	$A_V$	SFR <sub>SED</sub> $/M_\odot \text{yr}^{-1}$	SFR <sub>FIR1</sub> $/M_\odot \text{yr}^{-1}$	SFR <sub>FIR2</sub> $/M_\odot \text{yr}^{-1}$	SFR <sub>Rad</sub> $/M_\odot \text{yr}^{-1}$	SFR <sub>obs</sub> / SFR <sub>UV</sub>	sSFR $/\text{Gyr}^{-1}$
UDF1	$10.7 \pm 0.10$	$0.31 \pm 0.05$	3.1	399.4	$326 \pm 83$	$364 \pm 82$	$439 \pm 28$	$1052 \pm 317$	$6.50 \pm 2.24$
UDF2	$11.1 \pm 0.15$	$0.32 \pm 0.10$	2.2	50.2	$247 \pm 76$	$194 \pm 64$	$242 \pm 22$	$772 \pm 339$	$1.96 \pm 0.92$
UDF3 <sup>†</sup>	$10.3 \pm 0.15$	$4.70 \pm 0.30$	0.9	42.0	$195 \pm 69$	$173 \pm 1$	$400 \pm 17$	$41 \pm 15$	$9.77 \pm 4.88$
UDF4	$10.5 \pm 0.15$	$0.43 \pm 0.20$	1.6	20.0	$94 \pm 4$	$58 \pm 5$	$89 \pm 17$	$219 \pm 102$	$2.97 \pm 1.05$
UDF5	$10.4 \pm 0.15$	$0.20 \pm 0.05$	2.4	36.1	$102 \pm 7$	$67 \pm 25$	$86 \pm 6$	$510 \pm 132$	$4.06 \pm 1.46$
UDF6	$10.5 \pm 0.10$	$0.10 \pm 0.02$	2.8	78.0	$87 \pm 11$	$66 \pm 5$	$68 \pm 5$	$870 \pm 205$	$2.75 \pm 0.73$
UDF7	$10.6 \pm 0.10$	$0.50 \pm 0.03$	1.5	16.5	$56 \pm 22$	$77 \pm 42$	$617 \pm 20$	$112 \pm 45$	$1.41 \pm 0.64$
UDF8	$11.2 \pm 0.15$	$0.98 \pm 0.02$	1.6	35.8	$149 \pm 90$	$94 \pm 37$	$73 \pm 5$	$152 \pm 92$	$0.94 \pm 0.66$
UDF9	$10.0 \pm 0.10$	$0.06 \pm 0.01$	0.9	0.5	$23 \pm 25$	$5 \pm 2$	$5 \pm 1$	$383 \pm 421$	$2.30 \pm 2.56$
UDF10	$10.2 \pm 0.15$	$1.14 \pm 0.10$	1.5	37.0	$45 \pm 22$	$34 \pm 7$	$<35$	$39 \pm 20$	$2.84 \pm 1.71$
UDF11	$10.8 \pm 0.10$	$6.29 \pm 0.20$	1.4	162.8	$162 \pm 94$	$232 \pm 10$	$172 \pm 14$	$26 \pm 15$	$2.57 \pm 1.60$
UDF12	$9.6 \pm 0.15$	$1.55 \pm 0.10$	0.2	2.6	$37 \pm 14$	$21 \pm 7$	$<100$	$24 \pm 10$	$9.29 \pm 4.80$
UDF13	$10.8 \pm 0.10$	$0.95 \pm 0.05$	1.3	18.0	$68 \pm 18$	$60 \pm 19$	$142 \pm 17$	$72 \pm 19$	$1.08 \pm 0.38$
UDF14	$9.7 \pm 0.10$	$0.05 \pm 0.01$	1.3	1.0	$44 \pm 17$	$3 \pm 2$	$<4$	$880 \pm 383$	$8.78 \pm 3.96$
UDF15	$9.9 \pm 0.15$	$1.14 \pm 0.02$	1.1	15.5	$38 \pm 27$	$25 \pm 8$	$<20$	$33 \pm 24$	$4.78 \pm 3.79$
UDF16	$10.9 \pm 0.10$	$0.10 \pm 0.05$	0.6	0.5	$40 \pm 18$	$25 \pm 4$	$38 \pm 3$	$400 \pm 269$	$0.50 \pm 0.26$

↑ rest frame UV  
(1500Å)

↑ HUDF Template= ‘Best’  
↑ 6GHz

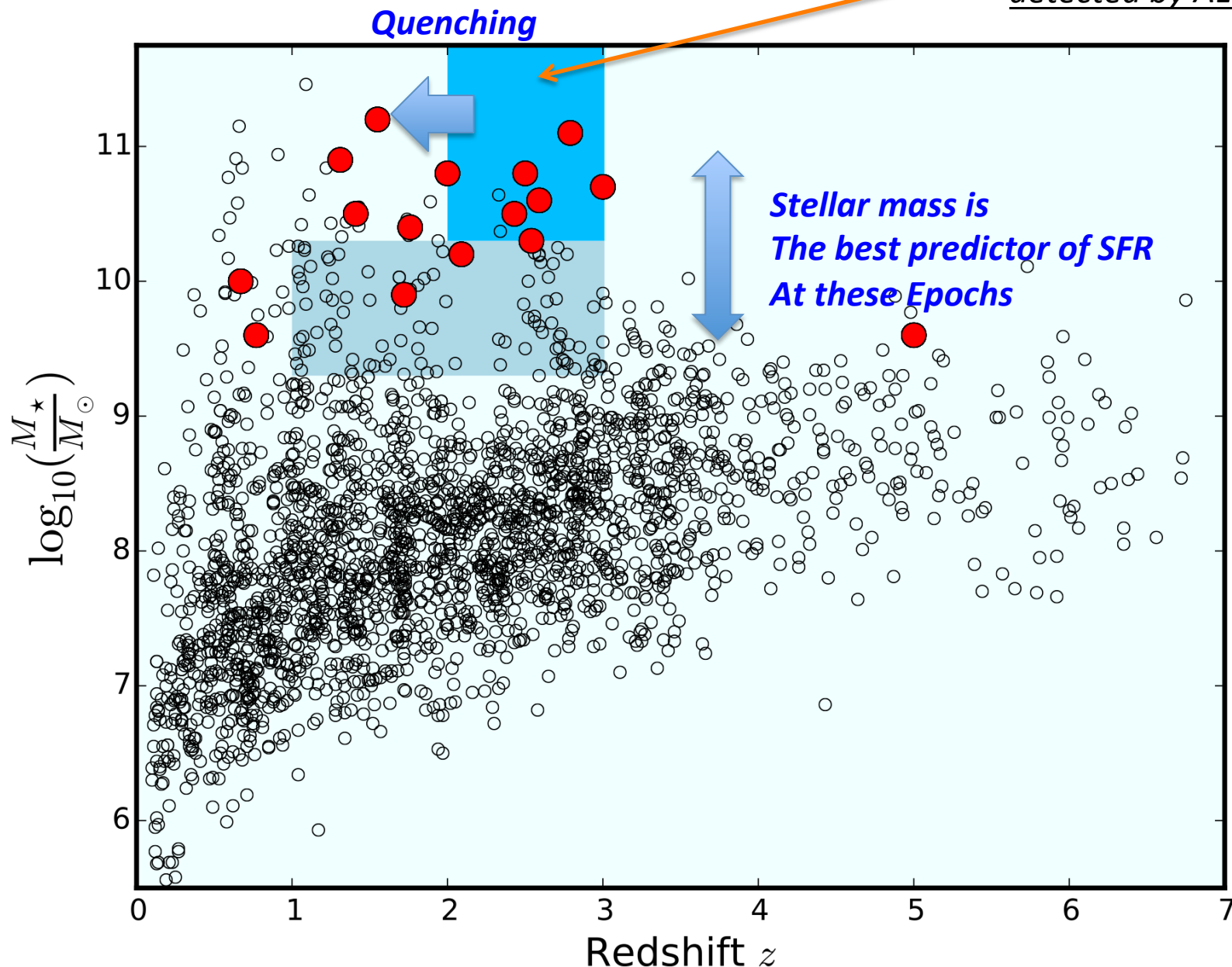
# Redshifts

- 13 spec-z + 3 photo-z
- The distribution is in very good agreement with classical SMGs.  
->  $\langle z \rangle = 2.15$   
13/16 are at  $z=1.5\text{-}3$ .
- only one detection beyond  $z=3.1$   
=> the absence of high-mass galaxies at these redshifts.
- the decline at  $z < 1.5$   
=> quenching of SF activity in high-mass galaxies.

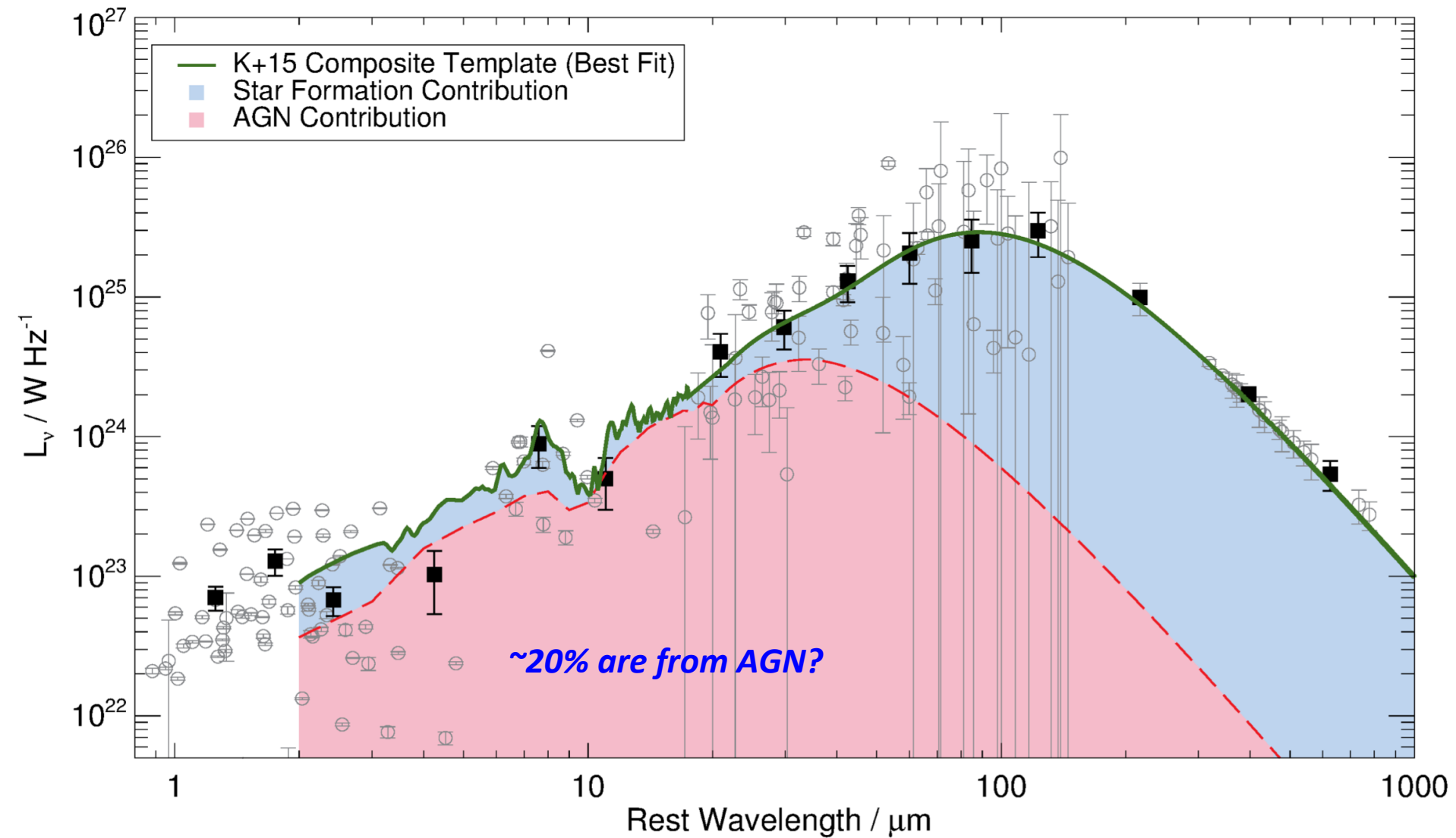


# Stellar Masses

7/9 are  
detected by ALMA!

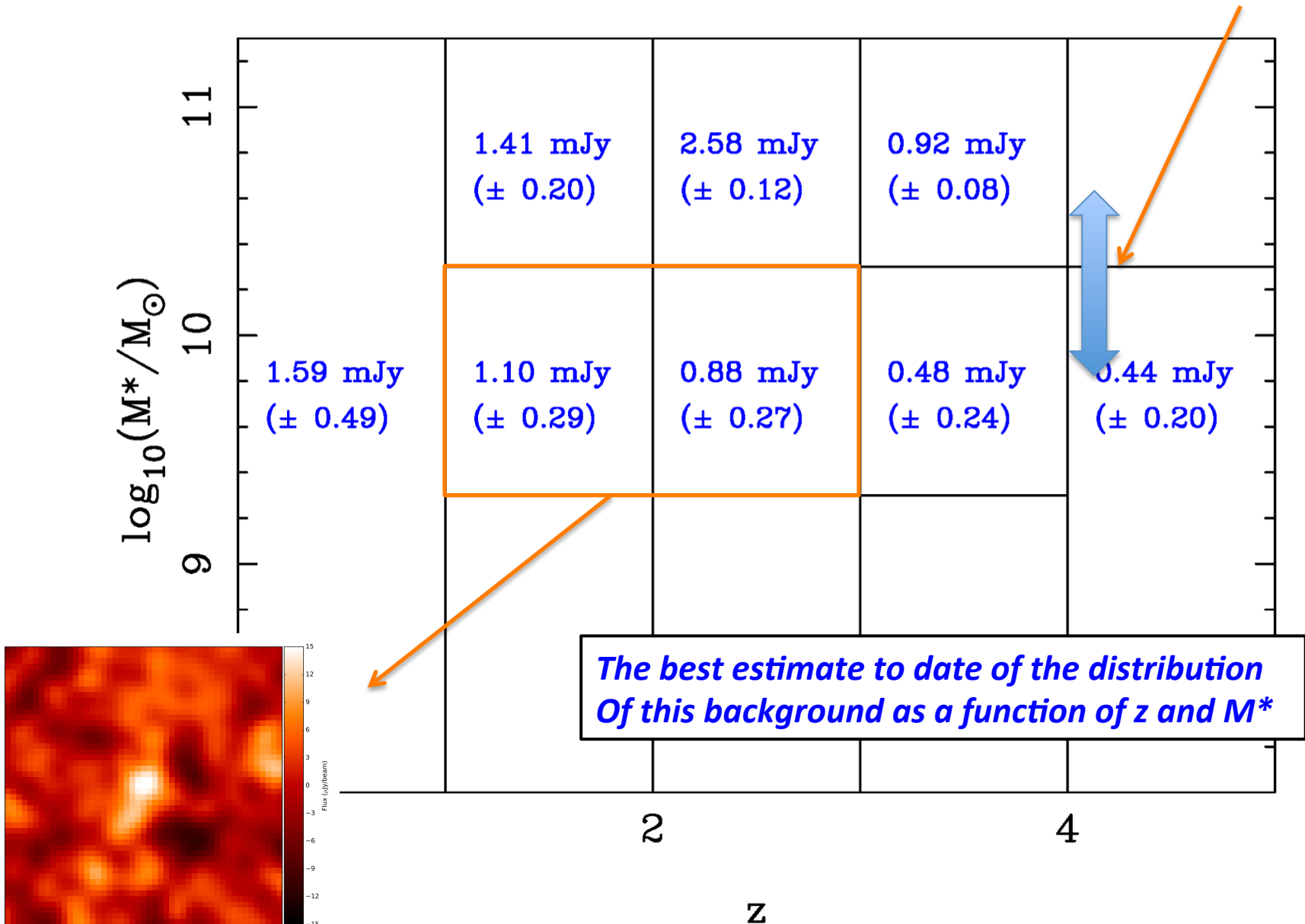


# Combined Templates

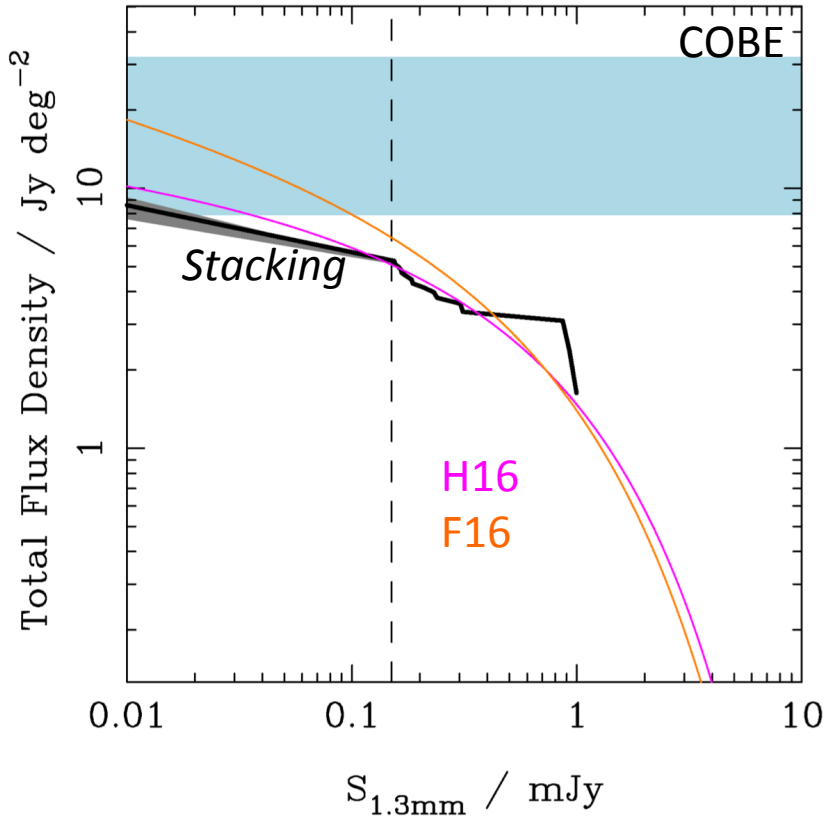
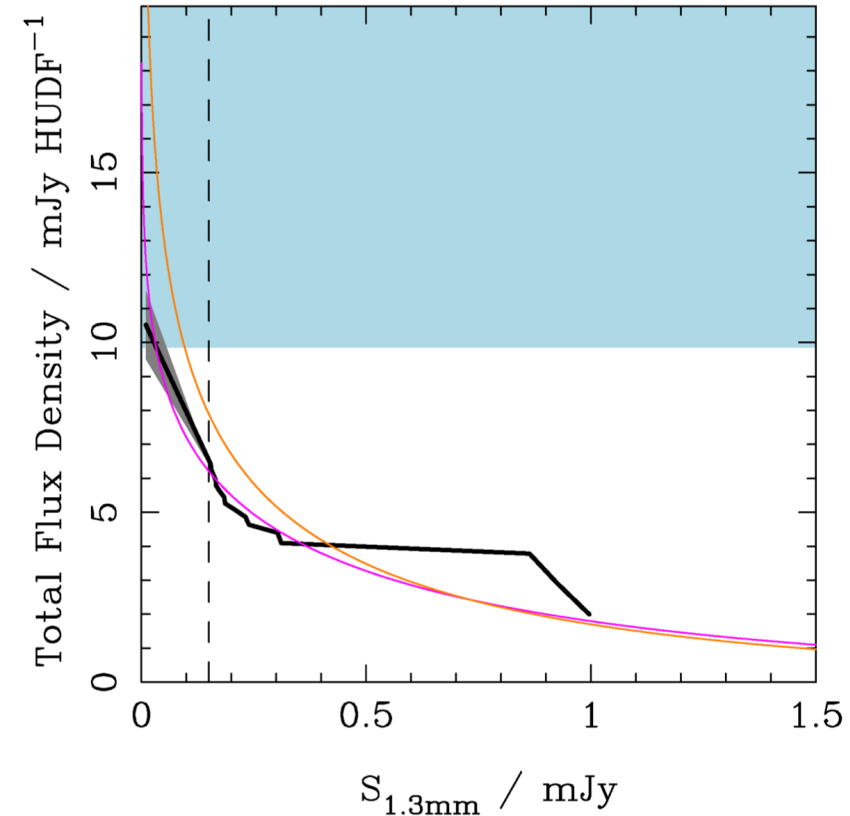


# Stacking Analysis

*The steep dependence of  
Dust-obscured SF on  $M^*$*

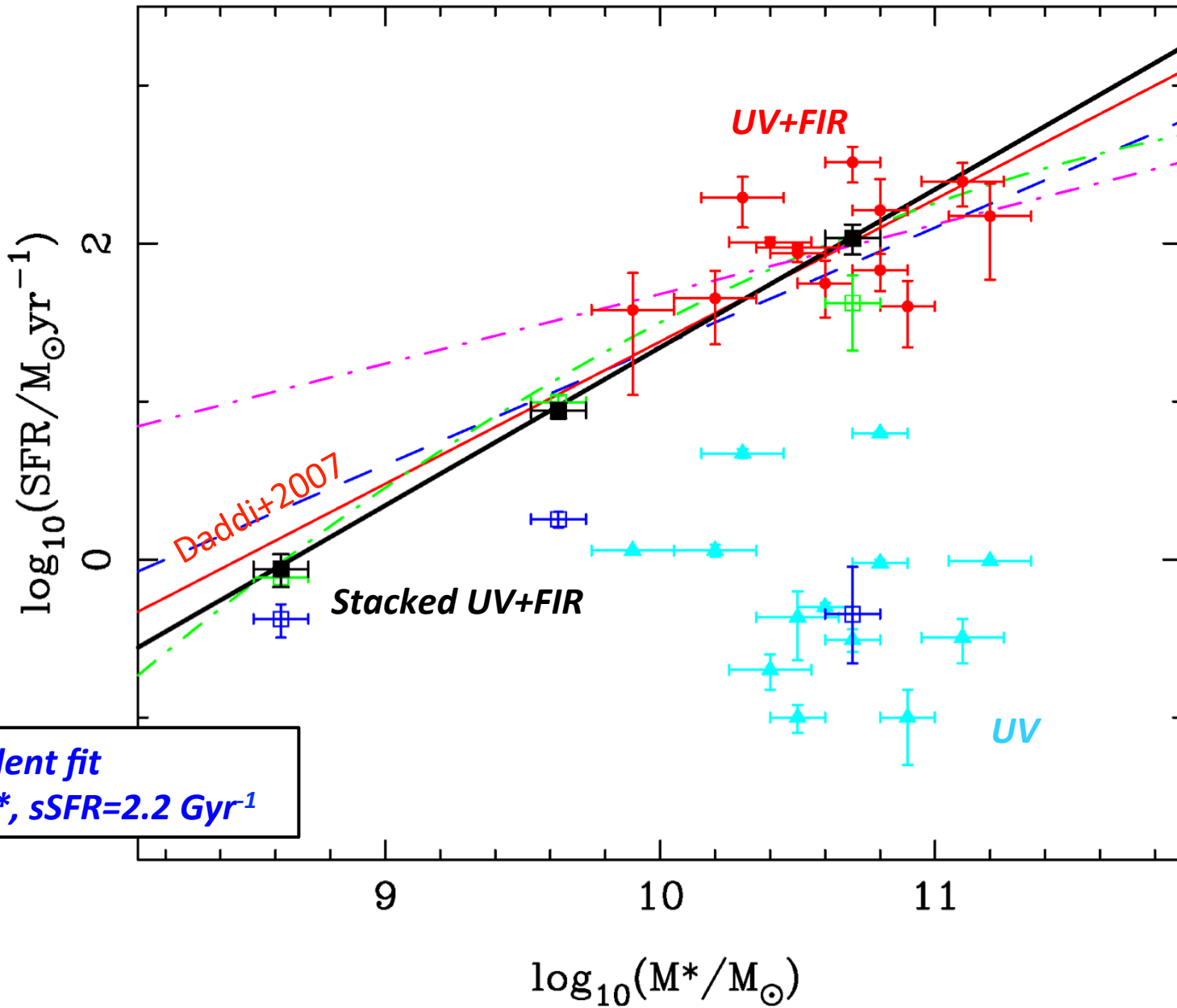


# EBL

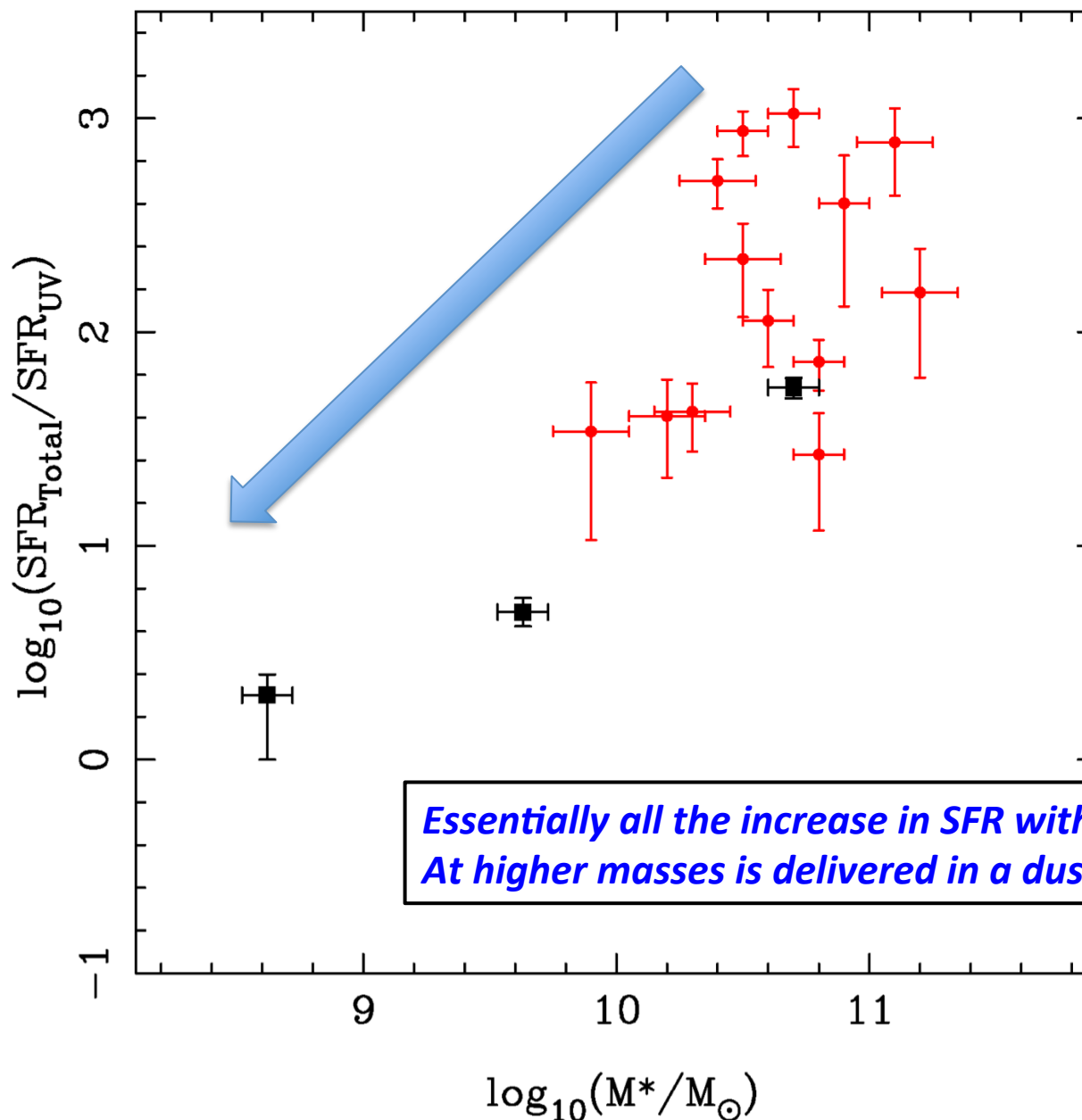


- consistent with the 1- $\sigma$  lower bound on the COBE estimate
- ‘we would require to approximately double the flux density in HUDF’

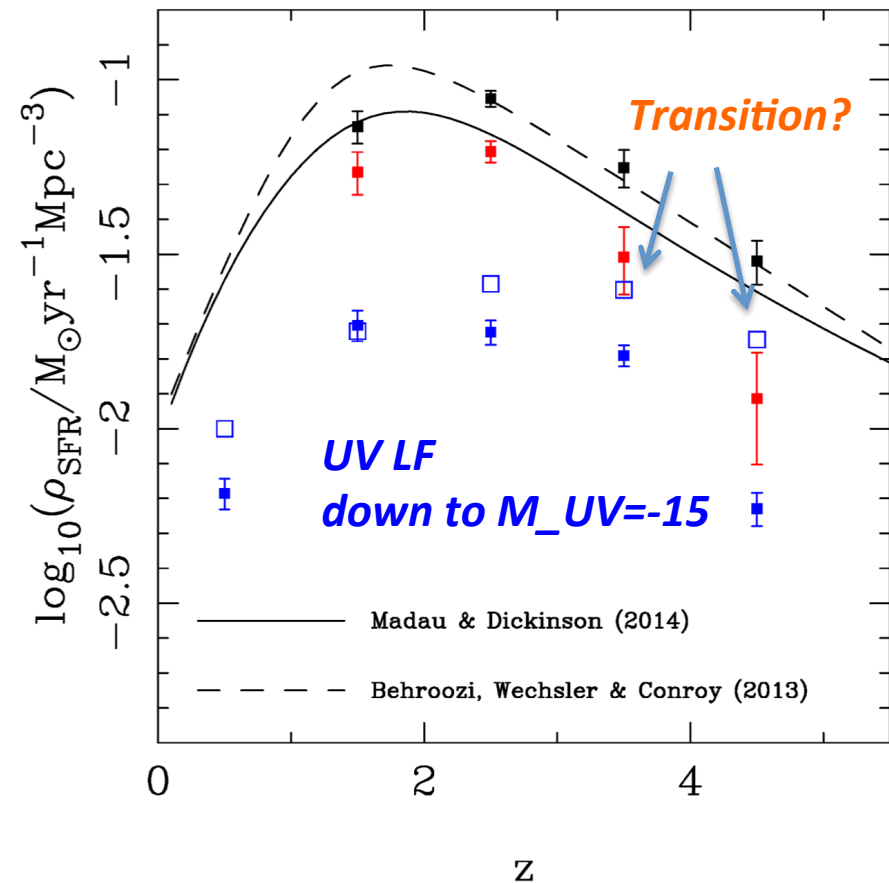
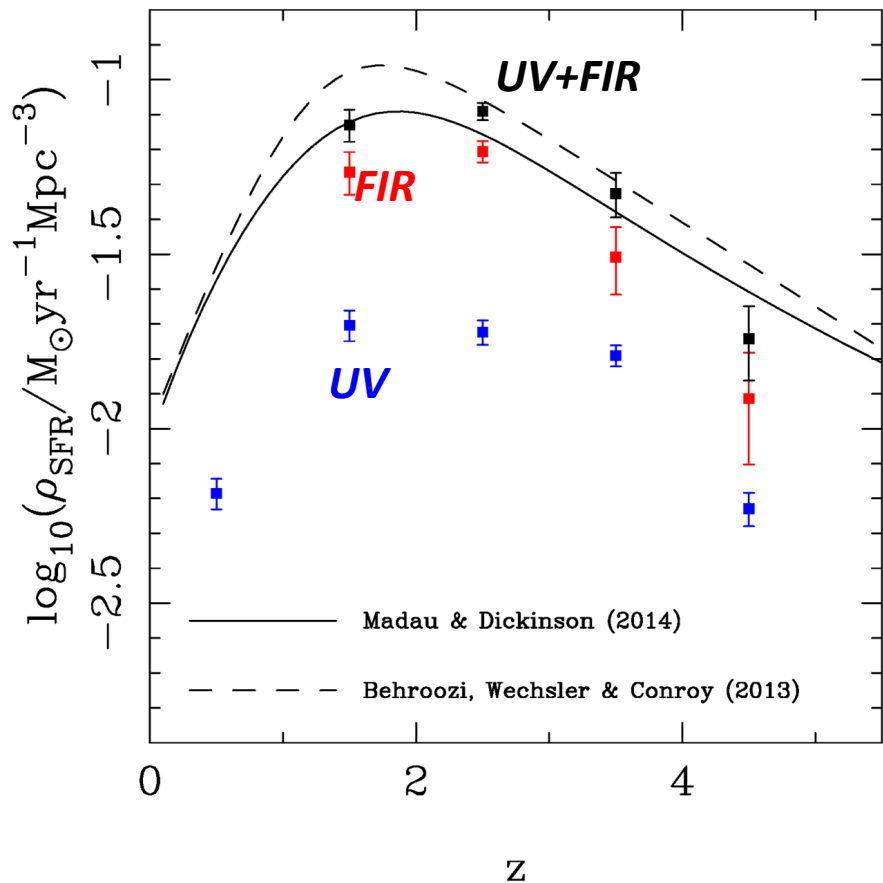
# The star-forming MS



# Obscured vs unobscured



# Cosmic star-formation history



- ‘This is the first time a direct census of  $\rho_{\text{SFR}}(\text{obscured})$  has been performed at these redshift.’
- At  $z > 4$ , most of the SF in the Universe is unobscured.

# Abstract

## ABSTRACT

We present the results of the first, deep ALMA imaging covering the full  $\simeq 4.5 \text{ arcmin}^2$  of the Hubble Ultra Deep Field (HUDF) as previously imaged with WFC3/IR on the *HST*. Using a mosaic of 45 ALMA pointings, we have obtained a homogeneous image of the HUDF at  $\lambda = 1.3 \text{ mm}$ , achieving an rms sensitivity  $\sigma_{1.3} \simeq 35 \mu\text{Jy}$ , at a resolution of  $\simeq 0.7 \text{ arcsec}$ . From an initial list of  $\simeq 50 > 3.5\sigma$  peaks, a rigorous analysis confirms 16 sources with flux densities  $S_{1.3} > 120 \mu\text{Jy}$ . All of these have secure galaxy counterparts with robust redshifts ( $\langle z \rangle = 2.15$ ), and 12 are also detected at 6 GHz in new ultra-deep JVLA imaging. Due to the wealth of supporting data in this unique field, the physical properties of the ALMA sources are well constrained, including, crucially, their stellar masses ( $M_*$ ) and UV+FIR star-formation rates (SFR). Our results show that stellar mass is the best predictor of SFR in the high-redshift Universe; indeed at  $z \geq 2$  our ALMA sample contains 7 of the 9 galaxies in the HUDF with  $M_* \geq 2 \times 10^{10} M_\odot$ , and we detect only one galaxy at  $z > 3.5$ , reflecting the rapid drop-off of high-mass galaxies with increasing redshift. The detected sources, coupled with stacking, allow us to probe the redshift/mass distribution of the 1.3-mm background down to  $S_{1.3} \simeq 10 \mu\text{Jy}$ . We find strong evidence for a steep ‘main sequence’ for star-forming galaxies at  $z \simeq 2$ , with  $\text{SFR} \propto M_*$  and a mean specific  $\text{SFR} \simeq 2.2 \text{ Gyr}^{-1}$ . Moreover, we find that  $\simeq 85\%$  of total star formation at  $z \simeq 2$  is enshrouded in dust, with  $\simeq 65\%$  of all star formation at this epoch occurring in high-mass galaxies ( $M_* > 2 \times 10^{10} M_\odot$ ), for which the average obscured:unobscured SF ratio is  $\simeq 200$ . Finally, we combine our new ALMA results with the existing *HST* data to revisit the cosmic evolution of star-formation rate density ( $\rho_{\text{SFR}}$ ); we find that  $\rho_{\text{SFR}}$  peaks at  $z \simeq 2.5$ , and that the star-forming Universe transits from primarily unobscured to primarily obscured thereafter at  $z \simeq 4$ .